Photos: Corbis, DOI: 10.2516/ogst/2012104, IFPEN, X.

Dossier

This paper is a part of the hereunder thematic dossier published in OGST Journal, Vol. 68, No. 6, pp. 951-1113 and available online here

Cet article fait partie du dossier thématique ci-dessous publié dans la revue OGST, Vol. 68, n°6, pp. 951-1113 et téléchargeable ici

DOSSIER Edited by/Sous la direction de : **C. Barrère-Tricca**

IFP Energies nouvelles International Conference / Les Rencontres Scientifiques d'IFP Energies nouvelles

MAPI 2012: Multiscale Approaches for Process Innovation

MAPI 2012 : Approches multi-échelles pour l'innovation des procédés

Oil & Gas Science and Technology – Rev. IFP Energies nouvelles, Vol. 68 (2013), No. 6, pp. 951-1113

Oil & Gas Science and Technology – Rev. IFP Energies nouvelles, Vol. 68 (2013), No. 6, pp. 1059-1072

DOI: 10.2516/ogst/2012085

IFP Energies nouvelles International Conference
Rencontres Scientifiques d'IFP Energies nouvelles

MAPI 2012: Multiscale Approaches for Process Innovation
MAPI 2012 : Approches multi-échelles pour l'innovation des procédés

Bubbles in Non-Newtonian Fluids: A Multiscale Modeling

X. Frank, J.-C. Charpentier, F. Cannevière, N. Midoux and H.Z. Li*

Laboratory of Reactions and Process Engineering, University of Lorraine, CNRS, 1 rue Grandville, BP 20451, 54001 Nancy Cedex - France
e-mail: huai-zhi.li@univ-lorraine.fr

* Corresponding author

Résumé — **Bulles en fluide non Newtonien : une approche multi-échelle** — Une approche multi-échelle de la dynamique des bulles en ascension dans un fluide non Newtonien est présentée. La vélocimétrie par imagerie de particules (PIV) et la simulation Lattice Boltzmann (LB) permettent de comprendre les caractéristiques de l'écoulement complexe autour d'une bulle isolée. Les interactions et coalescences entre bulles sont étudiées expérimentalement à l'aide de mesures de champ de vitesse par PIV et de visualisations du champ de contrainte par biréfringence autour de bulles isolées et de trains de bulles formés par un orifice immergé. Ces interactions sont gouvernées essentiellement par deux phénomènes : la création de contraintes liées au passage des bulles à travers le fluide, d'une part, et la relaxation de ces contraintes, d'autre part. Une dynamique non linéaire complexe résulte de la compétition entre ces deux phénomènes antagonistes. Un modèle dit « cognitif », construit à partir de règles comportementales, est déduit de la connaissance détaillée des phénomènes à l'échelle de la bulle et des mécanismes gouvernant le comportement à l'échelle mésoscopique. Les bulles sont modélisées comme les individus d'un système multiagents, interagissant entre eux *via* la contrainte résiduelle au sein du fluide. La prédiction des coalescences successives entre un grand nombre de bulles présente un bon accord avec les résultats expérimentaux à l'échelle macroscopique. D'importantes caractéristiques qualitatives et quantitatives du comportement collectif des bulles à l'échelle macroscopique sont prédites par la modélisation cognitive des interactions entre bulles à l'échelle mésoscopique, elle-même déduite de la connaissance des mécanismes à l'œuvre autour des bulles à l'échelle microscopique.

Abstract *— **Bubbles in Non-Newtonian Fluids: A Multiscale Modeling** — In this paper, the concept of a multiscale modeling approach is highlighted with which physical phenomena at different scales can be studied. The work reports a multiscale approach to describe the dynamics of a chain of bubbles rising in non-Newtonian fluids. By means of the Particle Image Velocimetry (PIV) and the Lattice Boltzmann (LB) simulation, a deep understanding of the complex flow pattern around a single bubble is gained at microscale. The interactions and coalescences between bubbles rising in non-Newtonian fluids are experimentally investigated by the PIV measurements, birefringence and rheological characterization for both an isolated bubble and a chain of bubbles formed from a submerged orifice. Two aspects are identified as central to interactions and coalescence: the stress*

creation by the passage of bubbles and their relaxation due to the fluid's memory. This competition between the creation and relaxation of stresses displays non-linear complex dynamics. Along with the detailed knowledge around a single bubble, these fundamental mechanisms governing bubbles' collective behavior in a train of bubbles at mesoscale lead to a cognitive modeling based on behavioral rules. By simulating bubbles as adaptive agents with the surround fluid via *residual stresses, model predictions for consecutive coalescence between a great number of bubbles compare very satisfactorily with the experimental investigation at macroscale.*

Obviously this new approach captures important quantitative and qualitative features of the collective behaviors of bubbles at macroscale level which are predicted by the mesoscopic cognitive modeling approach of the interactions rules which are deduced from the understanding of the microscopic mechanism of the flow around a single bubble.

NOTATION

C_D	Drag coefficient
$\vec{c}_i$	Lattice velocity
D_o	Orifice diameter (m)
$D_{\max}$	Maximum bubble diameter (m)
DPD	Dissipative Particle Dynamics
F	Force (N)
LB	Lattice Boltzmann
P	Pressure (Pa)
$P_{\alpha,\beta}$	Pressure tensor
Q	Gas flowrate ($m^3.s^{-1}$)
$\vec{r}$	Lattice location
T	Injection period between bubbles (s)
t	Time (s)
U, U'	Bubble rise velocity ($m.s^{-1}$)
$\vec{u}$	Fluid velocity ($m.s^{-1}$)
V_B	Bubble volume (m^3)

GREEK LETTERS

$\Gamma_{\alpha,\beta}$	Viscoelastic stress tensor
$\dot{\gamma}$	Shear rate (s^{-1})
η	Viscosity (Pa.s)
κ	Adiabatic coefficient
θ	Angle between the normal to the bubble surface at any element and the vertical axis
λ	Relaxation time in Carreau model (s)
λ_k	kth relaxation time in Maxwell model (s)
ρ_L	Fluid density ($kg.m^{-3}$)
ρ_G	Gas density ($kg.m^{-3}$)
σ	Surface tension ($N.m^{-1}$)
τ	Stress tensor
τ	Stress (Pa)
τ_r	Relaxation time (s)

INTRODUCTION

The bubble behaviors in non-Newtonian fluids are widely encountered in various domains such as decompression sickness, volcanic eruption, glass manufacture, materials, petrochemicals, metallurgy and different dispersed systems. In chemical engineering, typical examples of applications include waste water treatment, handling and processing of fermentation broths, polymer devolatilization, bubble column, mechanical stirrer with multiphase, enhanced oil and gas recovery, composites processing, plastic foam processing, etc. The efficiency of heat and mass transfer processes, and chemical or biological reactions is essentially governed by the collective behavior of numerous bubbles issued from a multihole distributor: flow field around a bubble; interactions and coalescence between bubbles; bubble size distribution in a column; gas holdup, etc. Also, there is a strong academic motivation towards developing a fundamental understanding of the detailed influence of the fluid's rheology on the bubble flow patterns.

In comparison to the state-of-the-art of bubbles in Newtonian fluids (Clift *et al.*, 1978), much less is known about the bubble behaviors in non-Newtonian fluids (Chhabra, 2006; Debregeas *et al.*, 1998; Hassager, 1979). Due to the inherent complex nature of bubble phenomena, a complete theoretical analysis is still impossible at present. An adequate understanding of the bubble hydrodynamics in such media is a prerequisite to studying the other transport phenomena like heat and mass transfer with or without chemical reactions. The bubble behaviors can be subdivided into distinct processes: bubble formation from submerged orifices, interaction and coalescence during the ascent. A simplified starting point has been the study of bubbles issued from a single submerged orifice. The first major work was reported by Astarita and Apuzzo (1965) on the motion of single bubbles. The investigation in this field has been followed by numerous authors (Fan *et al.*, 2010; Chhabra, 2006; Rodrigue, 2002; Funfschilling

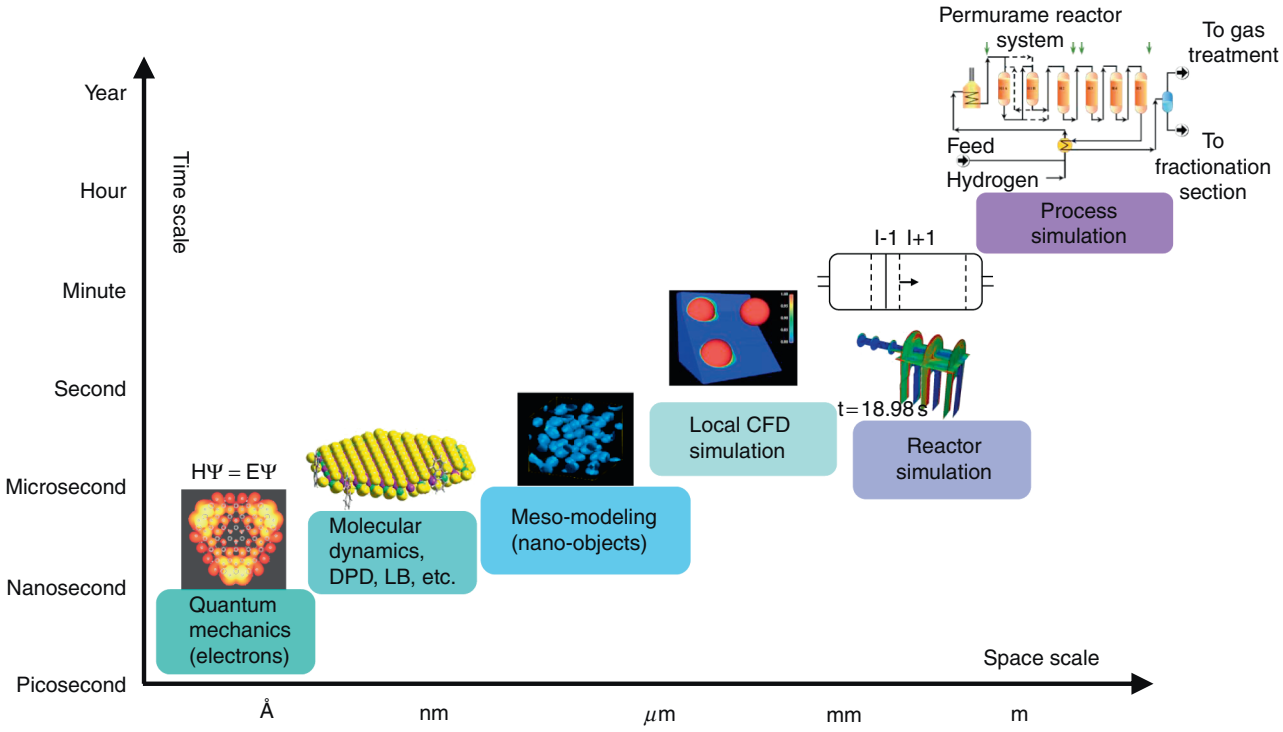

Figure 1

Illustrative view of a modern multiscale spatio-temporal approach in chemical engineering.

and Li, 2001; Haque *et al.*, 1987 for example). The results available in the literature provided essentially experimental information on the rise velocity of a single bubble or on the global hydrodynamics and mixing in a bubble column. In particular, a more detailed review on the effects of fluid's viscoelasticity on bubble shape and velocity can be found in the recent book of Chhabra (2006). Very few investigations on the interactions as well as coalescence between bubbles in such media have so far been reported in the literature (Lin and Lin, 2009; De Kee *et al.*, 1990; Acharya and Ulbrecht, 1978).

A major particularity of the aforementioned phenomena is the existence of a wide domain of both spatial and temporal scales at which different physical mechanisms happen. Furthermore, these mechanisms of different scales usually interact each other in a non-linear manner to lead to a huge variety of phenomena that underlines the complexity of the subject. Thus, as for the so proposed "*the molecular Processes-Product-Process Engineering (3PE) approach*" (Charpentier, 2010) to describe multidisciplinary non-linear and non-equilibrium phenomena occurring on different length and time scales in Chemical Engineering (*Fig. 1*), the bubble behaviors in non-Newtonian fluids could be dealt with an integrated system approach of multiscale modeling. The key idea is to understand how physical, chemical and interfacial phenomena at a fine scale relate to properties and behavior at a coarser scale step by step, *e.g.*, organizing levels of complexity (Frank *et al.*, 2012; Luo *et al.*, 2009; Charpentier, 2002).

In this work, we propose a philosophical approach to model the collective behaviors of bubbles in non-Newtonian fluids at different spatial and temporal scales: detailed information around a single bubble at microscale by both the fine experiments and numerical simulation; at mesoscale, interactions and coalescence laws issued from the detailed knowledge around a single bubble; some illustrative prediction results of macroscopic properties such as the bubble size distribution and comparison with the relative experiments at macroscale. Possible extension is discussed to take into account the interactions and coalescence between bubbles not only in line but also in parallel, for example in the presence of two orifices for the generation of bubbles.

1 EXPERIMENTAL

The experimental set-up was composed of cylindrical tanks in Plexiglas surrounded by a square duct (*Fig. 2*). The role of the square duct is to eliminate optical distortions for visualization as well as to control the

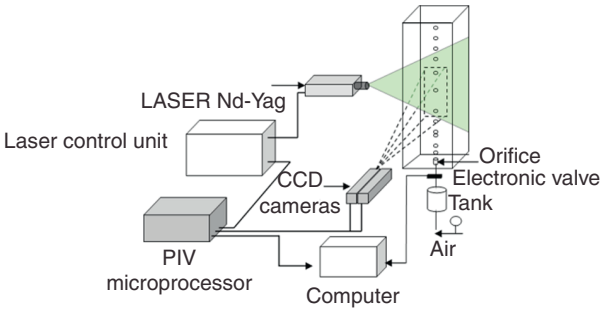

Figure 2

Experimental set-up with the PIV and lighting devices.

liquid temperature inside the cylindrical tank. The diameter of the tanks ranges from 0.20 m to 0.30 m and their height varies from 0.30 m to 1.50 m. Air and nitrogen bubble generation is through orifices of varying diameters ($1\text{-}5 \times 10^{-3}$ m), submerged in the liquid in the bottom section of the tanks. For the generation of bubbles from a single orifice, an electronic valve of rapid response controlled by a computer permits to inject bubbles of determined volume with desired injection period T in order to modulate the spatial distance between bubbles. Otherwise, it is always possible to inject bubble under a continuous gas flowrate without possibility to control the injection period between bubbles. The bubble rise velocity and the frequency of formation or passage are measured by laser probes at different heights. All experiments were carried out at constant temperature. The non-Newtonian fluids used in this work are different concentrations of polyacrylamide (PAAm) and of carboxymethylcellulose (CMC) in water or in water/glycerol mixtures. A Rheometrics Fluid Spectrometer RFS II and an AR 2000 rheometer (*TA Instruments*) were employed to measure the rheological properties. These fluids behaved as shear-thinning fluids and could be fitted for the whole range of the shear rates tested ($\dot{\gamma} = 0.01$ to 1 000 s^{-1}) by the Carreau model:

$$\frac{\eta - \eta_\infty}{\eta_0 - \eta_\infty} = \left[1 + (\lambda\dot{\gamma})^2\right]^{\frac{n-1}{2}} \quad (1)$$

For example, 0.50% PAAm has the following data: $\eta_0 = 38$ Pa.s, $\eta_\infty = 0.005$ Pa.s, $\lambda = 45.6$ s and $n = 0.29$.

Stress relaxation measurements show that at the same shear rate, the relaxation time ranges from 1 s for diluted CMC solutions to 45 s for concentrated PAAm solutions. Therefore, PAAm solutions may be seen much more elastic than CMC solutions. To describe the viscoelastic properties of this fluid, a 6th order Maxwell model is developed on the base of rheological measurements (Frank and Li, 2005b):

$$G(t) = \sum_{k=1}^{6} G_k \exp\left(-\frac{t}{\lambda_k}\right) \quad (2)$$

Instantaneous velocity fields around a bubble are measured by means of a Particle Image Velocimetry technique (PIV, *Dantec Dynamics*, Denmark) (*Fig. 2*). Illumination sheets are generated with two pulsed Nd-YAG Lasers (*New Wave Research*, USA) arranged side-by-side and cross the vertical symmetry axis of the dispersed phase. The energy produced by this source is 2×15 mJ. These lasers emit green light with a wavelength of 532 nm for a duration of 8 to 10 ns. The time between the flashes varies from less than one microsecond to a few milliseconds. The Nd-Yag lasers are also designed to ensure a sequence of illuminations at a frequency of 15 Hz. The laser beams first cross a cylindrical lens which gave a laser sheet of strong light intensity and small thickness (2 mm maximum). They are focused and superimposed on one zone of measurement. The fluids are inseminated with fluorescent polymer beads (Rhodamine B) of 50 μm as seeding particles. An orange filter placed in front of the camera eliminates the reflections of the lasers on the bubbles and lets only the fluorescent light of the particles pass. The size is determined to minimize both Brownian movement and seeding particle sedimentation. The camera, placed perpendicular to the laser sheets, takes two successive images at the maximum intensity of the laser pulse. These images are divided into a few thousand small interrogation areas of 16×16 pixels. A cross-correlation is then performed between the corresponding interrogation areas. When the flow is correctly inseminated, the measurement errors on the velocities are less than 5%. The visualization was carried out by two high-speed digital cameras (VNR 950, *Sysma Industrie*, France; CamRecord600, *Optronis GMBH*, Germany) at a rate ranging from 100 to 5 000 fps. The light is provided by a halogen light of 800 W, which enlightens the columns *via* indirect lighting on a white screen behind the bubble column.

2 MULTISCALE APPROACH AND RESULTS

2.1 Flow Around a Single Bubble: A Microscopic Description

The direct simulation of flow around a deformed bubble remains a challenging problem for computational multiphase flows. The need to explicitly model the dynamics

of the interface between different phases and the associated difficulties of adapting the computational grid used to compute the flow within each phase present tremendous challenges for conventional fluid simulation approaches. The Lattice Boltzmann method is a powerful technique for the computational modeling of a wide variety of complex fluid flow problems (Succi, 2001). Based upon the Boltzmann equation, this approach is a discrete computational method that considers a typical volume element of fluid to be composed of a collection of particles that are represented by a particle velocity distribution function for each fluid component at each grid point. The time is counted in discrete steps and the fluid particles collide with each other as they move. The rules governing the collisions are designed such that the time-average motion of the particles is consistent with the Navier-Stokes equation. Within the Lattice Boltzmann (LB) framework, the fluid is described at the molecular level in a statistical way. Molecules are forced to move on a lattice that is a discretization of the phase space. We used here the so-called D2Q9 lattice, a bi-dimensional lattice, on which particles' velocity can have only 9 values, including zero. Evolution of the system with the discrete time t consists in a streaming stage, where molecules move from their node and reach a neighboring node, and a collision stage, where molecules collide and velocities are consecutively modified. Molecules are not implemented directly but described in a statistical way by means of the Particle Probability Distribution Functions (PPDF) f_i, where $f_i(\vec{r},t)$ is the number of molecules having the velocity $\vec{c}_i$ at the point $\vec{r}$ and time t. Useful quantities are deduced from PPDF and molecules' velocities:

$$\rho = \sum_i f_i \tag{3}$$

$$\rho\,\vec{u} = \sum_i f_i \vec{c}_i \tag{4}$$

The time evolution of PPDF obeys the LBGK (Lattice Bhatnagar-Gross-Krook) equation that is nothing but a simplification of the general Lattice Boltzmann equation:

$$f_i(\vec{r}+\delta t\vec{c}_i, t+\delta t) - f_i(\vec{r},t) = -\frac{1}{\tau_r}(f_i - f_i^{eq}) + \frac{\vec{a}.(\vec{c}_i-\vec{u})}{c_s^2} f_i^{eq}\delta t \tag{5}$$

Distributions f_i^{eq} are equilibrium polynomial expression and computed with the following conserved quantities:

$$\sum_i f_i^{eq} = \rho$$

$$\sum_i f_i^{eq}\vec{c}_i = \rho\,\vec{u} \tag{6}$$

$$\sum_i f_i^{eq} c_{i\alpha} c_{i\beta} = \rho\, u_\alpha u_\beta + P_{\alpha,\beta} - \Gamma_{\alpha,\beta}$$

where $P_{\alpha,\beta}$ is the pressure tensor deduced from a free energy scheme (Frank *et al.*, 2006; Frank and Li, 2005b, 2006) and $\Gamma_{\alpha,\beta}$ the viscoelastic stress tensor that is computed with the help of a modified 6th order Maxwell model. The non-Newtonian properties of the fluids, including viscoelastic ones, were implemented in the LB scheme based on the modified Maxwell fluid coupled to shear-thinning effects. This rheological approach was dynamically validated through successive relaxation experiments (Frank and Li, 2005b, 2006).

To perform bubbly flow simulations at microscale, a gas-liquid model is required. The free energy-based model seems suitable to simulate bubbles in both Newtonian and non-Newtonian fluids (Frank *et al.*, 2006; Frank and Li, 2005b). To describe both hydrodynamics and multiphase patterns in binary fluids, two densities, ρ_A and ρ_B, are necessary with a total density $\rho = \rho_A + \rho_B$ and a density difference $\Delta\rho = \rho_A - \rho_B$. As ρ and $\vec{u}$ are implemented through PPDF f_i as in single phase flows, the density difference $\Delta\rho$ is computed from g_i, another PPDF functions obeying a LBGK equation too.

The flow fields around an individual bubble in these solutions have very peculiar features: the flow in the front of the bubble is very similar to that in the Newtonian case; in the central wake, the movement of the fluid is surprisingly downward; finally, a hollow cone of upward flow surrounds this negative wake. This conical upward flow zone begins on the sides of the bubble and is largely extended backward (*Fig. 3*). The real typical shape of the bubble is also added in Figure 3 to locate the position of the bubble. Obviously, the bubble's shape in the non-Newtonian fluids differs much from that in Newtonian case. Small bubbles are elongated vertically and have a teardrop shape. By further increase in volume, bubbles take the flattened shape however with always a tail behind the bubble. In the past, the negative wake was initially investigated by both the qualitative visualization (Sigli and Coutanceau, 1977) and the use of LDA (Hassager, 1979; Bisgaard, 1983) at a point in a non-Newtonian fluid; however, our results show clearly the global shape of the negative wake, in particular the conical upward flow zone around the negative wake. It is worth noting that the conical open angle θ decreases with the bubble's volume and tends to an asymptotic value in these fluids. These detailed flow patterns were extensively investigated by the PIV device in our group in function of the fluids' viscoelasticity

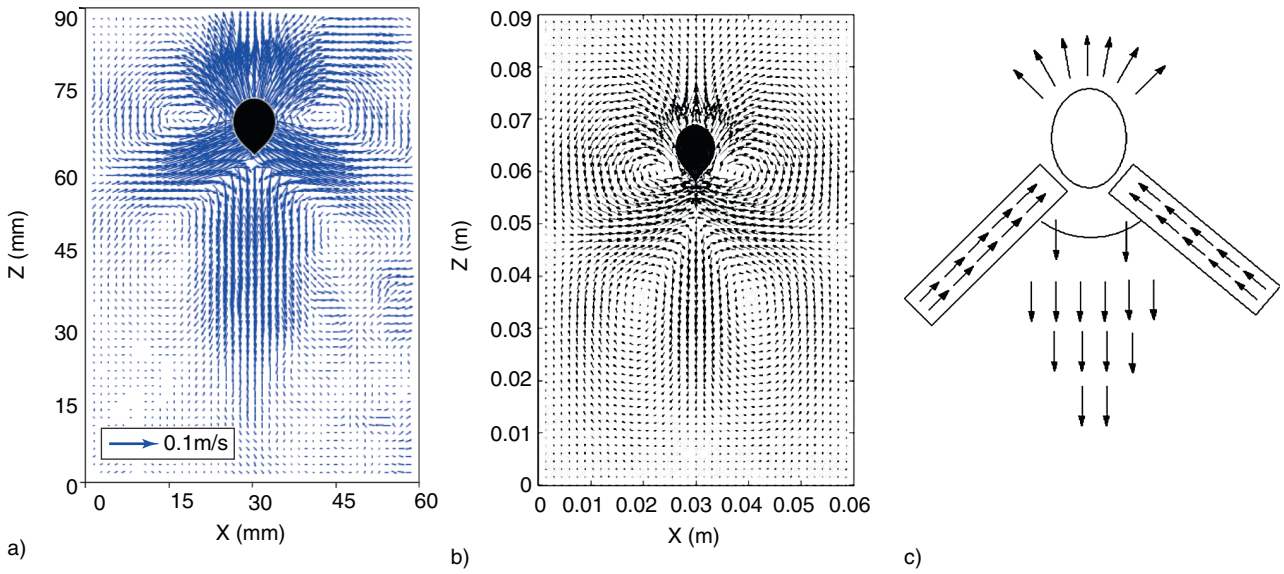

Figure 3

Flow field around a rising bubble of 190×10^{-9} m^3 in 1% (wt) PAAm solution. a) Experimental measurements by the PIV device. b) LB simulation with computed bubble shape. c) Schematic representation of the conical angle θ around a bubble rising in viscoelastic fluids.

(Funfschilling and Li, 2001; Frank *et al.*, 2003). The spatial distribution of stresses around a bubble between the conical ascension and the central negative wake was also quantified by the birefringence method. The fluid's viscoelasticity was identified as responsible for the origin of the negative wake (Kemiha *et al.*, 2006).

Figure 3a shows an experimental flow field, captured with the help of PIV device, and Figure 3b is a flow field from LB numerical simulation. The theoretical flow field exhibits effectively the negative wake, a conical positive flow around the negative wake with an open angle. The comparison with the experimental measurements is quite satisfactory, including the bubble shape simulated with the same model. However, a minor difference can be observed: recirculation is stronger in numerical case than in experiment. This could arise from the 2D simulation instead of 3D. The main advantage of the LB approach with respect to other numerical methods is the possibility to simulate very elastic fluids through the above-mentioned viscoelastic tensor. Moreover, the shape evolution of the bubble could also be computed as a direct consequence within the framework of a two-component and binary LB scheme. Clearly, both the high resolution about 50 μm of the PIV device and the microscopic equations used in the LB approach provide a solid foundation for understanding the various physical phenomena at microscale around a single bubble in non-Newtonian fluids.

2.2 In-Line Interactions and Coalescence Between Bubbles: Mesoscopic Modeling

2.2.1 In-Line Interactions Between Bubbles: A Linear Competing Mechanism of Stresses

With the help of the electronic valve controlled by a PC, we had the possibility to modulate the injection period T between two consecutive bubbles instead of the continuous injection of a gas flowrate. The evidence for in-line interactions between bubbles was clearly observed in this work: the rise velocity decreases with the increase of the injection period T for a given bubble volume. A sufficient long injection period is necessary to prevent the interactions between bubbles. When the injection period became short enough (< 1 s), the coalescence occurs. In particular, a significant factor differentiating bubble-bubble interactions in non-Newtonian fluids from that in water is the long field of action. So, we had the idea to simulate the passage of bubbles by imposing consecutive shear rates (pulses) to a fluid sample by means of the rheometer RFS II that measures the response of the sample in terms of shear stress. We call this original approach rheological simulation (Li *et al.*, 2004) that was performed in these fluids in the cone-and-plate geometry of the rheometer, taking especially into account the experimental values of rise velocity and injection period. There was a gradual accumulation of residual stresses tending asymptotically towards a

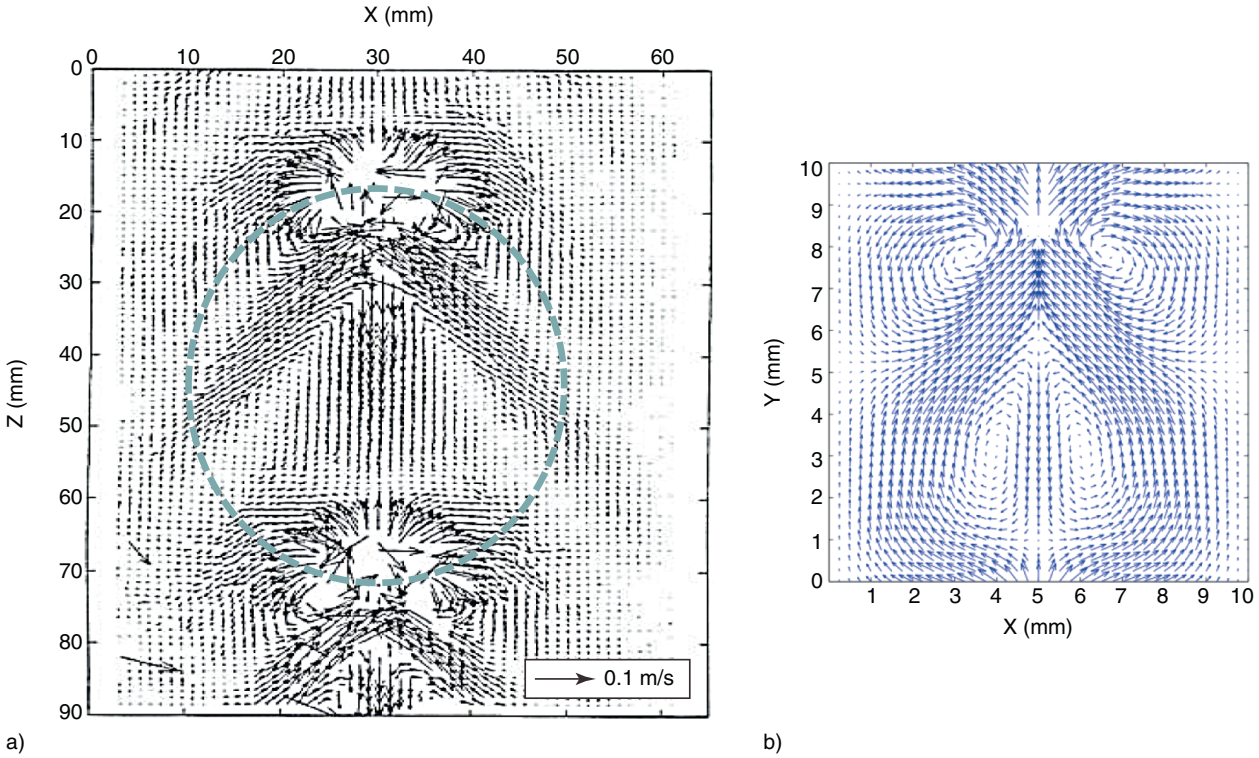

Figure 4

In-line interactions between a train of bubbles rising in 1% (wt) PAAm solutions. a) Flow field measured by the PIV and b) the LB simulation.

stationary value. The magnitude of these residual stresses could be considered as both strongly dependent upon the injection period and proportional to the elasticity of the fluid. It is clear that the trailing bubble can enter in the large field of residual stresses behind the leading one and provoke either interactions through pure acceleration of rise velocity or coalescence for closer intervals between bubbles.

Even if the flow field exhibits a negative wake behind a leading bubble as shown in Figure 4a by the PIV or Figure 4b by the LB simulation, the rise velocity increases for the whole train of bubbles. This flow configuration is totally different from that in Newtonian fluids. The wake hypothesis cannot explain the acceleration of bubbles, because it tends to suggest that bubbles will decelerate. These results suggest clearly that another mechanism should be discovered for interactions in non-Newtonian fluids. In the light of our several approaches, the following scenario can be proposed: after the passage of a leading bubble, the memory effect of the fluid holds the shear-thinning process during a certain time so that the local viscosity decreases and induces the acceleration of the rise velocity of the trailing bubble due to the reduced drag. The model is a continuous 1D average model. A column section-averaged field is defined for both velocity gradient and stress (Frank and Li, 2005a).

This memory effect of the residual stresses of preceding bubbles on the rise velocity of a bubble train is successfully modeled by means of the linear superposition principle to compute the acceleration of the rise velocity of a regular bubble train due to the temporary decrease of a local viscosity (*Fig. 5*).

2.2.2 Non-Linear and Chaotic Coalescence Between Bubbles: Cognitive Modeling

Above a critical threshold that depends on the viscoelastic nature of each fluid, the interactions are no longer linear as the coalescence occurs: a regular bubble chain is broken up (*Fig. 6*). The regularity of the bubble formation at the orifice (Li *et al.*, 2002) and the dynamical competition between the creation and relaxation of stresses lead naturally to the theory of chaos. We can recall the simplest competition that is a linear interaction. In order to understand the coalescence nature, the time delay embedding method of reconstructing the phase-space diagram was applied to time series data (bubble

passage) recorded at different heights in the bubble column. The calculation of several parameters: the largest Lyapunov exponent, the correlation dimension, the power spectrum and the phase portraits, indicates that the coalescence between bubbles is chaotic (Li *et al.*, 1997; Jiang *et al.*, 2011). Experimentally, the chaos' appearance can also be described by the period-doubling sequences. It is worth noting that the variation of the correlation dimension with the embedding dimension shows that the chaos is deterministic with a limited number of degrees of freedom. As shown in Section 2.3, this is also confirmed by the macroscopic evolution of the bubble number at different heights in the column. In fact, the bubble number normalized by the total number of bubbles generated at the orifice for a fixed duration (typically about 3 000 bubbles) levels off a plateau before falling due to the consecutive coalescence. The plateau corresponding to the constant bubble number in the inertial rise stage increases inversely with the fluid viscosity. The decrease of the bubble number in the higher column section is bounded by an asymptotic value due to the limited capacity of bubble generation at the orifice. This shows explicitly that the complexity of the in-line bubble coalescence in non-Newtonian fluids cannot degenerate into an arbitrary nature. Intuitively, the collective behaviors of bubbles in such media obey underlying fundamental laws.

The LB simulation could be applied to simulate the complex interactions between bubbles as shown in Figure 4b. However, it is worth noting that the LB is very CPU memory and time-consuming for the computation. A massive parallelization of the computation and the use of a supercomputer would be necessary. Recently, some physicists and biologists (Gell-Mann, 1994; Holland, 1992) are trying to explore a new way to describe the complex evolving systems such as an anthill, a central nervous system or ecosystems. Even though these complex systems differ in detail, the question of coherence under change is the central enigma for each. General principles rule usually the behavior of these Complex Adaptive Systems (CAS), principles that point to ways of solving the organizational problems. The task of formulating theory for these systems is more than difficult as the collective behavior of such a system is not a simple juxtaposition of the behaviors of its parts. The main quest is to extract these general principles and to shape them into building blocks for a new scientific approach.

To understand the interactions between large numbers of agents, we must be able to describe the capabilities of individual agents. It is quite logic to suppose that an agent's behavior is determined by some elementary rules. Stimulus-response rules are typical and simple: IF stimulus *S* occurs THEN gives response *R*. In an anthill, the stimuli could be pheromones deposed by other ants in search of foods, the response could be the moving

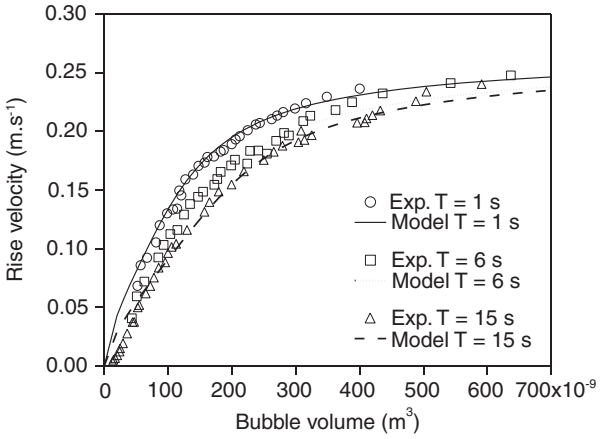

Figure 5

Comparison of the rise velocity of a bubble train between the theoretical linear modeling and experimental data in 0.5% PAAm with three injection periods without coalescence.

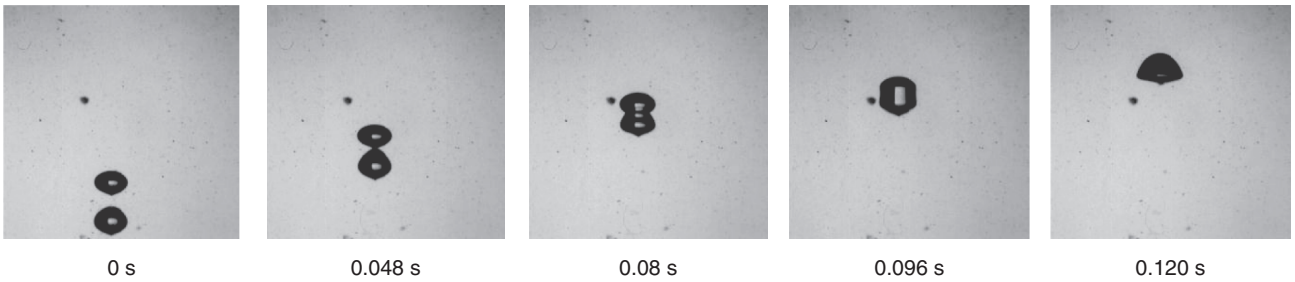

Figure 6

Coalescence between in-line rising bubbles.

direction according to the magnitude of pheromones. The collective behavior of the whole anthill would privilege the shortest way to go to the food source with progressive increase on the pheromones' intensity as each ant passing through this way would drop new pheromones. Therefore, we can establish qualitatively an ethnological analogy between bubbles and ants. They interact both between them through the interactions with their environment: pheromones for ants and residual stresses in fluid for bubbles. There is a connection between an ant and a bubble as an individual agent, as well as between the concentration of pheromones and the magnitude of stresses. This is experimentally confirmed by the injection of a sheared fluid through a syringe voluntarily displaced from the rise axe of the train of bubbles: due to the reduced viscosity in the sheared fluid, a rising bubble takes a bend to enter in the zone of reduced viscosity. The residual stresses left by this bubble guide the passage of trailing bubbles owing to the minimized drag and the modified rise axe can be self maintained as well as the displacement is not too large with respect to the initial vertical axe.

Our immediate objective is to find a simple syntax for IF/THEN rules that depend critically on the way an agent (a bubble) interacts with its environment (fluid) and other agents (bubbles). The three basic elements of this approach are a set of detectors, a set of IF/THEN rules and a set of effectors. The detectors represent the bubble's capacities for extracting information from its environment (residual stresses in fluid, presence of other bubbles); the IF/THEN rules describes its capacities for processing that information (accelerating or not the rise velocity, coalescence or not); and the effectors are its ability to act on the environment (leaving its own residual stresses according to its size). Both ants looking for food and bubbles rising in non-Newtonian fluids interact with all preceding individual entities through a continuous field. In the case of ants, the continuous field is a pheromone deposition concentration on soil related to the number of ants and the diffusion. The stress field in which decreased viscosity and reduced drag persist is the relevant field for bubbles. Bubble rise velocity depends upon this continuous field. On the other hand, IF/THEN strategy is used to introduce coalescences in the model. Moreover, cognitive modeling coupling with the LB is not direct as only simulations for a single bubble were carried out with the LB approach in present study.

The total fluid height is divided into 20 000 cells in which the stresses are continuously computed according to the passage of consecutive bubbles. Each cell represents a height of 75 μm for a liquid height of 1.50 m and is supposed to display homogenous stresses whose evolution is estimated by the dynamical competition between the creation (passage of bubbles) and relaxation of stresses (memory effects) of the first order. As a first approximation, the bubble is considered as spherical with an equivalent diameter d_{eq}. With an added mass, the motion equation of a bubble is described by a classical balance of different forces: inertial, buoyancy and drag forces:

$$\left(\rho_G + \frac{11}{16}\rho_L\right) V_B \frac{dU}{dt} \approx \frac{11}{16}\rho_L V_B \frac{dU}{dt} = F_b - F_t \qquad (7)$$

where the buoyancy force: $F_b = (\rho_L - \rho_G)\, V_B\, g$ and the drag force: $F_t = \frac{1}{2} A C_D \rho_L U^2$ with $A = \pi d_{eq}^2/4$. The drag coefficient C_D can be determined from a Reynolds number (Chhabra, 2006; Rodrigue, 2002) defined by an effective local viscosity as described below as well as a local rise velocity of the bubble.

After the passage of a preceding bubble, the memory effect of the fluid holds the shear-thinning process *via* a relaxing shear rate $\dot{\gamma}_m$ and a decreased viscosity η_m during a certain time so that the local drag decreases and induces the acceleration of the rise velocity of the trailing bubble. The estimation of the local effective viscosity is made through a virtually additional shear rate corresponding to the residual stresses:

$$\begin{cases} \tau = \eta_m \dot{\gamma}_m \\ \eta_m = \eta_\infty + (\eta_o - \eta_\infty)\left[1 + (\lambda\dot{\gamma}_m)^2\right]^{\frac{n-1}{2}} \end{cases} \qquad (8)$$

In the present study, we use simply, as a first approximation, the characteristic shear rate:

$$\dot{\gamma}_B = U/d_{eq} \qquad (9)$$

The sum of these two shear rates leads to an effective viscosity:

$$\eta_e = \eta_\infty + (\eta_o - \eta_\infty)\left\{1 + [\lambda(\dot{\gamma}_B + \dot{\gamma}_m)]^2\right\}^{\frac{n-1}{2}} \qquad (10)$$

Approximately, the decrease magnitude of an effective viscosity could range from 2 for a less viscoelastic fluid to 10 for a higher viscoelastic fluid with a short injection period. For a bubble rising initially at U, the main rules have then the form:

- IF (there are residual stresses in a cell τ) THEN (compute the new increased velocity U' *via* η_e);
- IF (two bubbles enter in contact) THEN (coalescence takes place to form a new bigger bubble $V_B = V_{B1} + V_{B2}$ and compute the new rise velocity U').

These rules are based on the physical mechanisms understood at mesoscopic level and could be hopefully expected to predict the interactions and coalescence between a great number of bubbles to come close to the industrial scale. In particular, the experimental results (Li *et al.*, 1997; Jiang *et al.*, 2011) show that the coalescence between bubbles rising in-line takes place easily in non-Newtonian fluids. The film drainage is mainly encountered in Newtonian fluids or for the lateral coalescence between bubbles in non-Newtonian fluids.

Rigorously, the relaxation is a very complex procedure in polymer solutions. The cognitive approach employed in this study is to make use of averaged value of a temporarily relaxed local viscosity in the wake of a preceding bubble, instead of a complex and detailed local flow fields. Otherwise, the computation for the interactions and coalescence between great numbers of bubbles will be excessively time-consuming.

2.3 In-Line Interactions and Coalescence Between Bubbles in a Bubble Column: Macroscopic Properties

Instead of dealing with the complexity of interactions and coalescence between a great number of bubbles rising in a bubble column at macroscopic scale, the mesoscopic interactions rules deduced from the understanding of the microscopic mechanisms are then applied to follow numerically the ascension of 3 000 bubbles consecutively generated at the orifice in a bubble column filled up with a fluid of 1.50 m height. The total fluid height is represented by 20 000 individual rectangular cells as the simulation box. As the inlet condition, identical bubbles are regularly injected through an orifice at the bottom of the column with the experimental values of the period T. For the outlet condition, a bubble reaching the top of the column is eliminated for the following time step. A simple counter allows us to impose periodic bubbling in the numerical simulation. The coalescences take place when two bubbles get in touch due to the acceleration of the rise velocity of a trailing bubble with the reduced drag. These two bubbles form then a bigger one according to the mass conservation and its new rise velocity is computed with the new coalesced size.

The computation is implemented on a PC and several statistical quantities are stored at different heights in the column. Some illustrative results are given as follows in the 0.5% PAAm solution. Figure 7a shows a comparison of the local bubble number normalized by 3 000 injected at total at different heights between the experiments and the computing from the mesoscopic cognitive approach. The global tendency is well described by this approach even though the local curve details aren't perfect. The small difference results essentially in the mean values used of α and β for bubbles of different size instead of more accurate values for each size. With respect to the orifice, a minimum height that depends on the viscoelasticity is required to accumulate sufficient residual stresses to induce the first coalescence. With the increasing sequence of coalescences between bubbles, the number of bubbles decreases significantly with the height. In contrary, the bubble size increases due to the consecutive coalescences. Figure 7b represents the evolution of the bubble diameter

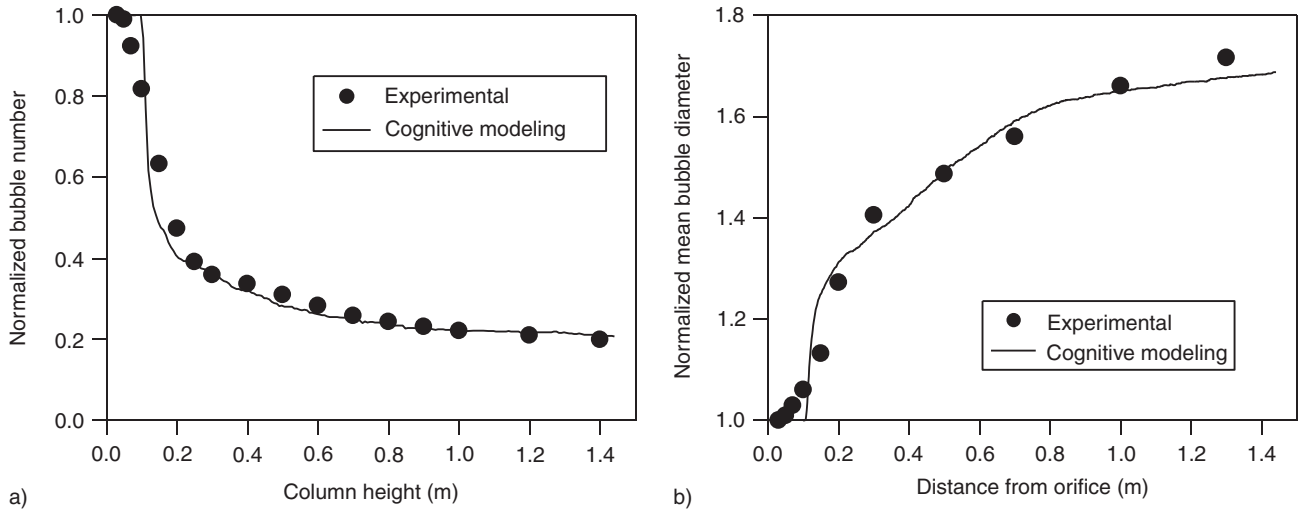

Figure 7

Comparison between the experiments and cognitive modeling in 0.5% (wt) PAAm solution for 3 000 bubbles. a) Variation of the normalized bubble number with the column height. b) Increase of the normalized bubble diameter with the column height.

normalized by the initial one in function of the fluid height. It is interesting to note that both the bubble number and the bubble diameter tend to asymptotic values as stated before; this indicates indirectly a bounded complexity due to mainly a constant injection flowrate of gas at the orifice as a limited resource, then a signature of deterministic chaos. These macroscopic behaviors predicted by the mesoscopic cognitive approach are particularly noteworthy as they emerge naturally without special fitting. These macroscopic data are indispensable for the design, operation and improvement of an industrial installation through the local knowledge on the bubble size distribution, gas holdup, specific interfacial area, etc. Detailed numerical intermediate values allow also signal treatments, for example, application of wavelets, bifurcation sequence analysis, route to chaos.

2.4 Parallel Interactions and Coalescence Between Bubbles

Obviously, the above-mentioned modeling approach is limited to the dynamics of a single rising train of bubbles. In industrial reality, the multihole distributor injects numerous trains of bubbles, rising not only in line but also in parallel. The mutual interactions and eventual coalescences between lateral bubble trains should then be included in the multiscale approach. A significant consequence of such interactions and coalescences is a possible deviation from an initial vertical trajectory of a train of bubbles to pinch two trains of bubbles issued from two neighboring orifices. Figure 8 shows such an interaction scenario: two bubbles pinch to get progressively closer. In the absolute majority, these bubbles slide to rise in line one after another. Usually, the in line coalescence takes place as in a unique train of bubbles (*Fig. 9a*). Very few lateral coalescences were observed during our experiments (*Fig. 9b*), probably due to the lateral shape of bubbles that is spherical. A point-to-point contact between two bubbles doesn't favor the drainage of the liquid film separating two bubbles and their coalescence.

As for the single bubble train, pairwise bubble-bubble lateral long-range interactions and short-range coalescences were monitored using a high-speed camera and

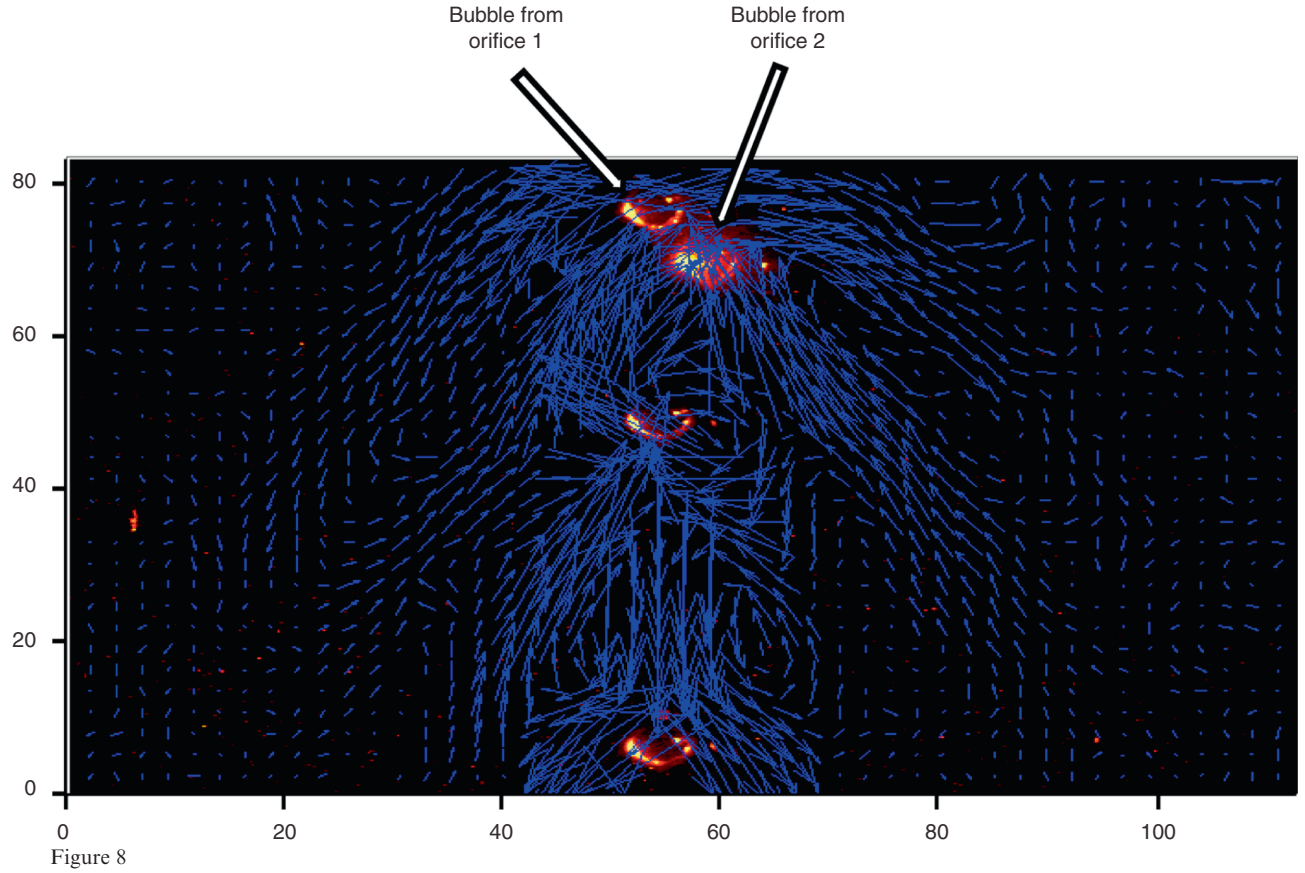

Figure 8

Flow fields around two laterally coalescing bubbles issued from two orifices by the PIV in 0.75% (wt) PAAm solution.

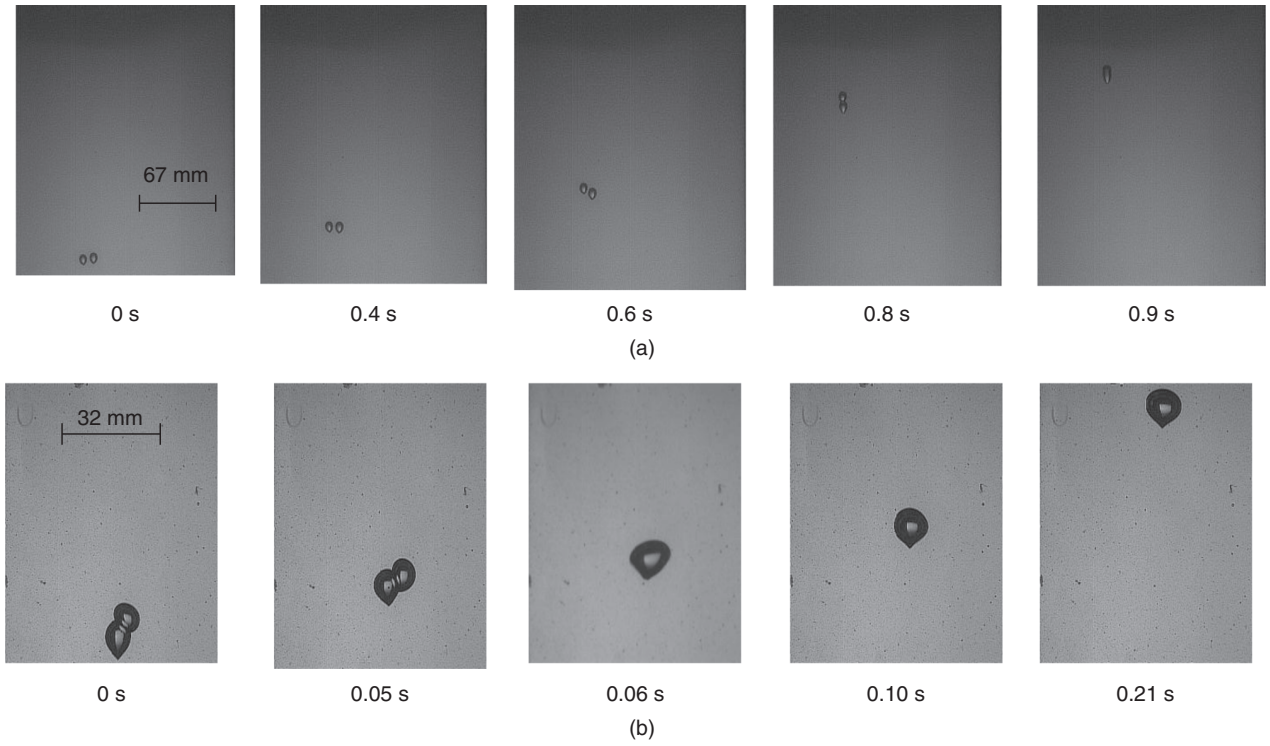

Figure 9

Interactions and coalescence between two trains of bubbles issued from two neighboring orifices in1% (wt) PAAm solutions. a) Dominant case: in line coalescence. b) Scarce case: coalescence in parallel.

the flow fields around bubbles during these interactions were quantified using our PIV device. Figure 8 shows the flow fields around two laterally coalescing bubbles issued from two orifices in parallel. With respect to a single orifice, two bubble trains from two orifices introduce lateral coalescences between bubbles trains, in addition to the in-line coalescences. The aim of such a bubble-scale study is to identify various scenarios of lateral interactions coalescences and to understand how the complex flow field features like negative wake and residual stresses privilege one scenario between several elementary processes. The philosophical concept is again based on the ethnological analogy with a well-organized society such as an anthill obeying some collective interacting rules: if there is a shortcut on the passage to collect foods or in the presence of predators, ants through the concentration of pheromone will adopt a decision-making by choosing the shortest or safest way (Mallon and Franks, 2000). For bubbles rising in non-Newtonian fluids, the reduced drag due to the residual stresses left by other bubbles is certainly the main rule to guide the passage (space occupation) of bubbles. Theoretically, it should be possible to describe interacting bubbles between them and with their fluid environment *via* residual stresses in terms of IF/THEN rules. The temporary passage signals of bubbles were monitored by the laser probes after the pinch of two bubble trains through optical probes. These signals reflect the number of bubbles passing before the probes located at different positions in the column. Even if the exact coalescence scenario requires better physical understanding, the signal analysis of the passage signals would provide some insight into the collective dynamics. The comparison between the cognitive modeling and the experiments is performed by means of spectral analysis in the Fourier's domain to reveal the dynamical characters such as chaotic behavior. However, the scenarios for lateral coalescence seem more complex and this is an avenue that we are currently exploring.

CONCLUSIONS AND DISCUSSIONS

Based on the swarm cognition, the concept of a multiscale modeling approach is highlighted for bubbles rising in non-Newtonian fluids in this paper in view of

simulating an industrial bubble column one day. A coherent picture begins to emerge on the bases of fundamental physical understanding at different scales. By means of both the experimental PIV and the Lattice Boltzmann simulation based on the particle dynamics, the detailed flow and stress features around a single bubble in different viscoelastic fluids are well understood at microscale. The proposed LB scheme interfaced with a viscoelastic model captures successfully the main flow features such as the complex negative wake, its physical origin, the bubble's teardrop shape and the spatial stress distribution around a bubble rising in a non-Newtonian fluid. These various fine experimental tools such as the PIV device, rheological stimulus-response simulation and the signal analysis of the temporary bubble passage at different heights are also applied to the investigation of one or two trains of bubbles at mesoscale with the main focus on the nature of interactions and coalescences between bubbles. The dynamical competition between the creation of stresses after the passage of bubbles and the relaxation of these stresses forming temporarily a corridor of reduced viscosity is clearly identified as the principal mechanism governing the in-line interactions and coalescences. Along with the detailed information gained by both the experiments and theoretical LB simulation, this knowledge on an in-line train of bubbles is resumed as interacting behavioral laws at mesoscale. An ethnological similitude can be drawn for the communicating agents between them through interactions with their environment: the evolution of the pheromone concentration deposed by ants on a favored passage in an anthill; the residual stresses left by the passed bubbles to guide trailing bubbles through a drag reduction in the fluid. Good agreement of the simulation results with experimental data is achieved for a train of numerous bubbles rising in a column at macroscale for various operating parameters at different heights such as the bubble number, mean bubble diameter, bubble class distribution, etc.

These results elucidate then the nature of in-line interactions and coalescence between bubbles rising in line in viscoelastic non-Newtonian fluids. However, it is still far from an industrial bubble column where great populations of bubbles rise, interact and coalesce not only in line but also in parallel. Further studies are then required to include this lateral spatial dimension in the multiscale modeling approach. We begin the study of interactions and coalescences between two trains of bubbles issued from two neighboring orifices. It seems that the chain-chain distance is the major control parameter for the intensity of lateral interactions and coalescences. However, the coalescence or not between two bubbles at the pinch point needs more detailed investigation. Besides extensive experiments under various conditions, a 3D LB simulation with parallelized codes is unavoidable to make use of powerful clusters and to keep computing time short enough, each CPU thread being devoted to a small part of bubble population in the column. It is envisaged that the present study could lay the foundation for a better comprehension and modeling of bubbles' collective dynamics with interfacial phenomena in these complex media at industrial scale.

REFERENCES

Acharya A., Ulbrecht J. (1978) Note on the influence of viscoelasticity on the coalescence rate of bubbles and drops, *AIChE J.* **24**, 348-351.

Astarita G., Apuzzo G. (1965) Motion of gas bubbles in non-Newtonian liquids, *AIChE J.* **11**, 815-820.

Bisgaard C. (1983) Velocity fields around spheres and bubbles investigated by laser-Doppler anemometry, *J. Non-Newton. Fluid Mech.* **12**, 283-302.

Charpentier J.C. (2002) The triplet "molecular processes-product-process" engineering: the future of chemical engineering? *Chem. Eng. Sci.* **57**, 4667-4690.

Charpentier J.C. (2010) Among the trends for a modern chemical engineering, the third paradigm: the time and length multiscale approach as an efficient tool for process intensification and product design and engineering, *Chem. Eng. Res. Des.* **88**, 248-254.

Chhabra R.P. (2006) *Bubbles, Drops & Particles in Non-Newtonian Fluids*, 2nd ed, CPC Press, Boca Raton.

Clift R., Grace J.R., Weber M.E. (1978) *Bubbles, Drops and Particles*, Academic Press, New York.

De Kee D., Chhabra R.P., Dajan A. (1990) Motion and coalescence of gas bubbles in non-Newtonian polymer solutions, *J. Non-Newton. Fluid Mech.* **37**, 1-18.

Debregeas G., de Gennes P.G., Brochard-Wyart F. (1998) The life and death of bare viscous bubbles, *Science* **279**, 1704-1706.

Fan W.Y., Ma Y.G., Jiang S.K., Yang K., Li H.Z. (2010) An experimental investigation for bubble rising in non-Newtonian fluids and empirical correlation of drag coefficient, *Trans. ASME J. Fluids Eng.* **132**, 021305.

Frank X., Li H.Z. (2005a) An analytical approach to the rise velocity of periodic bubble chains in non-Newtonian fluids, *Eur. Phys. J. E* **16**, 29-35.

Frank X., Li H.Z. (2005b) Complex flow field around a bubble rising in non-Newtonian fluids, *Phys. Rev. E* **71**, 036309.

Frank X., Li H.Z. (2006) Negative wake behind a sphere rising in viscoelastic fluids: a lattice Boltzmann investigation, *Phys. Rev. E* **74**, 056307.

Frank X., Funfschilling D., Midoux N., Li H.Z. (2006) Bubbles in a viscous liquid: Lattice Boltzmann simulation and experimental validation, *J. Fluid Mech.* **546**, 113-122.

Frank X., Charpentier J.C., Ma Y.G., Midoux N., Li H.Z. (2012) A multiscale approach for modelling bubbles rising in non-Newtonian fluids, *Ind. Eng. Chem. Res.* **51**, 2084-2093.

Frank X., Li H.Z., Funfschilling D., Burdin F., Ma Y. (2003) Bubble motion in non-Newtonian fluids and suspensions, *Can. J. Chem. Eng.* **81**, 483-490.

Funfschilling D., Li H.Z. (2001) Flow of non-Newtonian fluids around bubbles: PIV measurements and birefringence visualization, *Chem. Eng. Sci.* **56**, 1137-1141.

Gell-Mann M. (1994) *The Quark and the Jaguar: Adventures in the Simple and the Complex*, Wiley.

Haque M.W., Nigam K.D.P., Joshi J.B., Viswanathan K. (1987) Studies on mixing time in bubble columns with pseudoplastic solutions, *Ind. Eng. Chem. Res.* **26**, 82-86.

Hassager O. (1979) Negative wake behind bubbles in non-Newtonian liquids, *Nature* **279**, 402-403.

Holland J.H. (1992) *Adaptation in Natural and Artificial Systems: An Introductory Analysis with Applications to Biology, Control and Artificial Intelligence*, 2nd ed., MIT Press.

Jiang S.K., Ma Y.G., Fan W.Y., Yang K., Li H.Z. (2011) Fractal and chaotic behaviour of bubble coalescence in non-Newtonian fluids: a multiscale analysis, *Korean J. Chem. Eng.* **28**, 56-63.

Kemiha M., Frank X., Poncin S., Li H.Z. (2006) Origin of the negative wake behind a bubble rising in non-Newtonian fluids, *Chem. Eng. Sci.* **61**, 4041-4047.

Li H.Z., Frank X., Funfschilling D., Diard P. (2004) Bubbles' rising dynamics in polymeric solutions, *Phys. Lett. A* **325**, 43-50.

Li H.Z., Mouline Y., Choplin L., Midoux N. (1997) Chaotic bubble coalescence in non-Newtonian fluids, *Int. J. Multiphase Flow* **23**, 713-723.

Li H.Z., Mouline Y., Midoux N. (2002) Modelling the bubble formation dynamics in non-Newtonian fluids, *Chem. Eng. Sci.* **57**, 339-346.

Lin T.J., Lin G.M. (2009) Mechanisms of in-line coalescence of two-unequal bubbles in a non-Newtonian fluid, *Chem. Eng. J.* **150**, 750-756.

Luo K.H., Xia J., Monaco E. (2009) Multiscale modelling of multiphase flow with complex interactions, *J. Multiscale Modelling* **1**, 125-156.

Mallon E., Franks N. (2000) Ants estimate area using Buffon's needle, *Proc. R. Soc. Lond. B* **267**, 765-770.

Rodrigue D. (2002) A simple correlation for gas bubbles rising in power-law fluids, *Can. J. Chem. Eng.* **80**, 289-292.

Sigli D., Coutanceau M. (1977) Effect of finite boundaries on the slow laminar isothermal flow of a viscoelastic fluid around a spherical obstacle, *J. Non-Newton. Fluid Mech.* **2**, 1-21.

Succi S. (2001) *The Lattice Boltzmann Equation for Fluid Dynamics and Beyond*, Clarendon Press, Oxford.

Manuscript accepted in November 2012
Published online in June 2013